Soft Matter

Dynamic Article Links

Cite this: *Soft Matter*, 2012, **8**, 2599

www.rsc.org/softmatter

PAPER

The impact of ceramides NP and AP on the nanostructure of *stratum corneum* lipid bilayer. Part I: neutron diffraction and ^{2}H NMR studies on multilamellar models based on ceramides with symmetric alkyl chain length distribution

Tanja N. Engelbrecht,[a] Annett Schroeter,*[a] Thomas Hauß,[b] Bruno Demé,[c] Holger A. Scheidt,[d] Daniel Huster[d] and Reinhard H. H. Neubert[a]

Received 23rd February 2012, Accepted 11th April 2012
DOI: 10.1039/c2sm25420d

We investigated the lamellar structure of ternary *stratum corneum* (SC) lipid model systems based on either the phytosphingosine type ceramide (CER) [NP] or CER[AP], supplemented by cholesterol and stearic acid as representative free fatty acid species. For the CER[NP] based membrane, neutron diffraction measurements revealed the coexistence of two lamellar phases, which markedly differ in their hydration properties. CER[NP] forms an extremely rigid and stable bilayer backbone and is at least partly sequestered in a separate phase which coexists with a second lamellar phase. At increased temperature, a structural re-organization of the lipids was observed. One of the lamellar phases disappeared, while the remaining phase *increased* its repeat distance by about 1 Å. Such a behaviour has not been described for SC lipid model membranes based on CER[AP] so far. Further, ^{2}H NMR spectroscopic measurements on two SC lipid model systems based on either CER[NP] or CER[AP] in addition to cholesterol and perdeuterated stearic acid revealed a state of high lamellar order present in both samples, emphasizing the importance of the phytosphingosine-type ceramides for the proper formation of stable SC bilayer structures. However, the CER[NP] based ternary model showed a state of higher lamellar order than the CER[AP] based system. Our results demonstrate that slight changes in the ceramides' head groups (CER[NP] with 3 hydroxyl groups *vs.* CER[AP] with 4 hydroxyl groups) have a dramatic influence on the morphology of the lipid structures formed by these lipids.

1. Introduction

It is well known that the outermost layer of the mammalian skin, the *stratum corneum* (SC) maintains homeostasis of the organism by protecting the body from various outer influences and uncontrolled water loss. With its intercellular lipid matrix surrounding the corneocytes, the SC is generally accepted to represent the major penetration barrier of the skin.[1–3] Main constituents of the lipid lamellae are ceramides (CERs) in addition to cholesterol (CHOL) with its derivatives and free fatty acids (FFA),[4,5] whereby particularly the structural arrangement of these SC lipids in highly ordered and coherent multiple bilayers is regarded to be essential for the maintenance of the skin barrier properties.[6] The CERs represent a very lipophilic and rigid class of molecules with only small hydrophilic head groups, and they presumably determine the structure of the lipid lamellae of the SC to a high extent, which results *e.g.* in poor penetrability of mammalian skin for water.[6] Accordingly, it was found that there is almost no free water present inside the intercellular lamellar sheets of the SC.[7] With their particular properties, the CER lipids are regarded to be highly important for the proper formation of the penetration barrier.

Current SC research increasingly addresses the issue of identifying specific CER subclasses or SC lipid species playing a key role in the processes of skin barrier formation. There have been numerous attempts to correlate different states of impaired skin with alterations in the content of particular lipid species as reviewed previously.[8] For the case of atopic dermatitis, a significant reduction in the linoleic-acid containing ω-acylceramide CER[EOS] was found.[9] The authors concluded an important role of this CER subspecies for the skin barrier properties. Di Nardo and co-workers likewise reported a diminished content of ω-acyl-ceramides in the skin of atopic dermatitis patients[10] as well as a reduced CER[NP] level, which was assumed to account for the impaired transepidermal water loss observed for this unphysiological skin state. A strong reduction of the phytosphingosine-based CER[AP] and CER[NP] has also been demonstrated for the psoriatic skin.[11]

[a]*Institute of Pharmacy, Martin Luther University, Wolfgang-Langenbeck-Straße 4, 06120 Halle, Germany. E-mail: annett.schroeter@pharmazie.uni-halle.de; Tel: +49 345 25025*
[b]*Institute Soft Matter and Functional Materials, Helmholtz-Zentrum-Berlin, Hahn-Meitner-Platz 1, 14109 Berlin, Germany*
[c]*Institut Laue-Langevin (ILL), 6 Rue Jules Horowitz, 38042 Grenoble Cedex 9, France*
[d]*Institute of Medical Physics and Biophysics, University of Leipzig, Härtelstraße 16-18, 04107 Leipzig, Germany*

From the physicochemical point of view, the phytosphingosine-type CERs show distinct characteristics.[12,13] It was reported that CER[NP] is capable of forming an extremely strong network of intra- and inter-molecular hydrogen bonds,[12] which accounts for its distinct conformational characteristics and alkyl chain packing behaviour. When comparing the phytosphingoid-type CER[AP] and CER[NP] with sphingosine-based CERs, phase transition temperatures, intermolecular interactions and especially hydrogen bonding networks involving the hydrophilic head groups differ markedly.[14,15] The authors reasoned that it is the CER head group, which significantly determines the overall behaviour of the studied ternary lipid mixture.

Furthermore, the number and exact position of the hydroxyl groups in the hydrophilic head of the CER molecules was recognized to affect the intermolecular lipid interactions. The additional α-hydroxyl group present in CER[AP] was found to induce a certain sterical hindrance to the stabilizing hydrogen bond network mediated by the other hydroxyl groups of the CER head.[16] Consequently, there seems to be a sensitive balance of mutual interaction contributing to the stability of the overall SC lipid structure.

The protruding role of phytosphingosine-type CER[AP] for the formation of stable bilayer structures was also described in the work of Kiselev and co-workers.[17,18] Direct structural insights into the bilayer architecture of a CER[AP]-based quaternary SC lipid model membrane obtained from neutron diffraction revealed the formation of an extremely stable lamellar backbone with only little free water being present in the intermembrane space. Even under excess hydration, the repeat distance of the model bilayers only increased marginally by about 1 Å. The authors concluded that the polar CER[AP] accounts for the creation of such a rigid bilayer structure by forming strong lateral hydroxyl bonds, which was summarized in the armature reinforcement model. In the fully extended conformation, CER[AP] is assumed to pull the lamellae together, thereby preventing stronger swelling of the bilayers.[17] That work furthermore emphasized the importance of the non-destructive neutron diffraction technique for the purpose of structural investigation of lamellar structures. Additionally, the results obtained by further neutron diffraction experiments underlined that detailed information regarding the specific impact of particular CER species on the lamellar SC lipid assembly can favourably be received by studying simplistic SC model membranes based on mixtures of synthetic SC lipids featuring well-defined head group architecture and defined alkyl chain lengths.[19,20]

In order to advance our knowledge regarding the influence of phytosphingosine-type CERs on the molecular assembly of SC lipids, the present study focused on highly oriented ternary model membranes based on CER[NP] with symmetric alkyl chain length (stearic acid amide-bound to C18 phytosphingosine base), CHOL and the FFA stearic acid (SA). The system was investigated by means of neutron diffraction at two different temperatures in order to elucidate the bilayer architecture under varying environmental conditions. Additional ^{2}H NMR spectroscopic measurements were performed to study the structure and dynamics of the free SA in the mixture with CHOL and either CER[AP] or CER[NP] in order to analyze potential differences between CER[AP] or [NP] based systems.

2. Experimental

2.1. Materials

CER[NP] (*N*-(octadecanoyl)-phytosphingosine) and CER[AP] (*N*-(α-hydroxyoctadecanoyl)-phytosphingosine) were a gift of Evonik Goldschmidt GmbH (Essen, Germany). Since the substances had a purity of ≥96%, they were used as received without any further purification. CHOL and SA were purchased from Sigma Aldrich GmbH (Taufkirchen, Germany) and used as received. The perdeuterated SA (SA-d_{35}) used for ^{2}H NMR measurements was received from Dr Ehrenstorfer (Augsburg, Germany) and used without further purification. Cholesterol-25,26,26,26,27,27,27-d_7 was purchased from Avanti Polar Lipids (Alabaster, AL, USA). Quartz slides (Spectrosil 2000, 25 × 65 × 0.3 mm^3) for the neutron diffraction experiments were purchased from Saint-Gobain (Wiesbaden, Germany). Fig. 1 displays the chemical structure of the SC lipids used for the experiments. For the deposition of the lipids onto the quartz surface, an airbrush instrument (Harder & Steenbeck, Norderstedt, Germany) was employed. Chloroform and methanol used as solvents for preparation of the lipid solutions were of analytical grade. All buffer substances were obtained from Sigma Aldrich.

2.2. Sample preparation

2.2.1 Neutron diffraction experiment. Oriented multilamellar model membranes for investigation by means of neutron diffraction were prepared according to the procedure described earlier.[21] The sample studied by neutron scattering was composed of CER[NP]/CHOL/SA, component mass ratio (m/m) 55/25/20. A total volume of 1.2 ml of the final lipid mixture dissolved in chloroform/methanol (2 : 1 v/v) with a concentration of 10 mg ml^{-1} was spread over the quartz surface using the airbrush device at constant air flow. The solvent was allowed to evaporate under atmospheric pressure and subsequently under

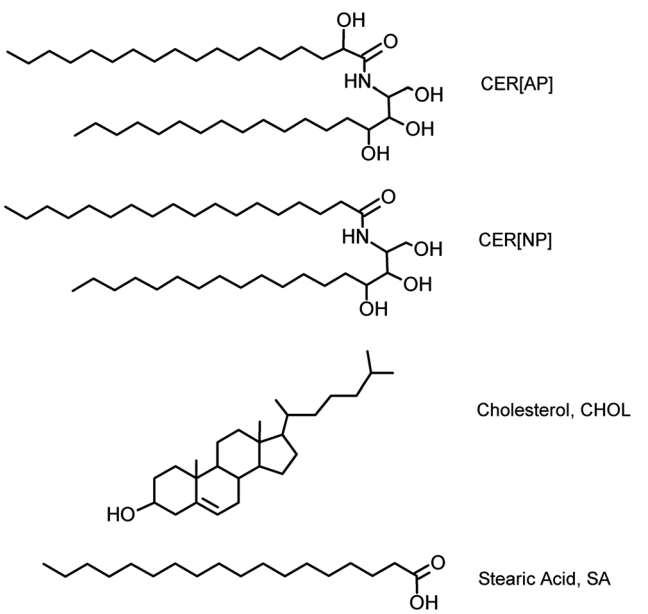

Fig. 1 The chemical structures of the SC lipids prepared as multilamellar SC model membranes.

reduced pressure (<50 mbar), where the samples were kept for 10–12 hours. After the solvent was removed completely, a subsequent annealing procedure was applied, whereby the samples were heated to 80 °C and cooled down to room temperature in water-saturated atmosphere. Such a procedure is often used in sample preparation for neutron diffraction experiments in order to improve the sample quality and state of lamellar order,[22] which is of benefit for the peak intensities in the diffraction experiment and for the subsequent data analysis. For a detailed description of the necessity of the annealing procedure see former reports.[23] Until the measurements, the samples were stored at room temperature.

2.2.2 ^{2}H NMR spectroscopy. For the ^{2}H NMR measurements, the sample composition was either CER[NP] or CER[AP] in mixture with CHOL and SA at a mass ratio (m/m) of 55/25/20, where either the stearic acid (SA-d_{35}) or the cholesterol (CHOL-d_7) was deuterated. Briefly, aliquots of the synthetic SC lipids were dissolved in chloroform/methanol 2 : 1 (v/v) and mixed in the required ratio to yield a total amount of 2.5 mg per sample. After the solvent was evaporated under vacuum (~1 mbar), the remaining lipid film was dispersed in 4 ml of an aqueous buffer solution (10 mM Hepes, 100 mM NaCl, pH 7.4). In order to achieve homogeneity, the lipid dispersion was heated up to 80 °C and shaken for 3 hours with alternating bath ultrasonication and extensive vortexing. The resulting homogeneous lipid dispersion was treated by ultracentrifugation (T = 4 °C, 79 000 × g) (Beckman Optima L-60, Beckman Coulter GmbH, Krefeld, Germany) in order to separate and remove excessive buffer. The samples were subjected to several freeze–thaw cycles to improve homogeneity, and finally transferred into 5 mm glass vials for NMR measurements.

2.3. Neutron diffraction experiments

The neutron diffraction experiments were performed at the Small Momentum Transfer Diffractometer D16 situated at the cold source of the High-Flux Reactor (HFR) at Institute Laue-Langevin (ILL, Grenoble, France). The neutron wavelength of λ = 4.74 Å used for our experiment was received by appropriate positioning of a pyrolytic graphite monochromator. A two-dimensional position-sensitive detector (^{3}He, area 256 × 256 mm^2, spatial resolution 2 × 2 mm^2) was used to record the scattered neutron intensity. Diffraction data were collected as rocking scans (ω-scans) with the samples being rocked around the expected Bragg positions ω while the detector was set to a fixed position 2θ at a sample-to-detector distance of 101.5 cm. For equilibration and subsequent measurements, the sample was mounted in lockable chambers. Parameters like temperature (T) and relative humidity (RH) were externally controlled. Prior to each measurement, the sample was equilibrated at a temperature of 32 °C (comparable to *in vivo* conditions) and the respective RH until no changes in peak intensity or peak position were detectable. According to previous studies, 6–8 hours are sufficient for equilibrium hydration of such SC lipid model membranes and consequently, this time period was also applied in the present experiment.[18] Measurements were performed at different temperatures, *i.e.* at 32 °C and 80 °C, and under relatively dry and more humid atmospheres (58% RH and 99% RH, respectively). The comparatively high temperature of 80 °C was chosen to investigate the behaviour of the ternary model membrane near the main phase transition temperature. Since liquid-crystalline lipid bilayers are known to be several-fold more permeable for agents than gel-state lamellar structures,[24] it is important to study the structural properties of the SC lipid model lamellae in the liquid-crystalline state.

For each measurement condition, the model membrane was studied at no less than three different D_2O contrasts in order to vary the neutron scattering length density between the lipids and water. For that purpose, the chamber atmosphere was set to three D_2O/H_2O concentrations: 100/0, 50/50 and 8/92 (mol/mol).

The multilamellar sample was exposed to a monochromatic and collimated incoming neutron beam during measurements, while the intensity of scattered neutrons I was recorded as a function of the scattering angle 2θ. The correlation of 2θ to $\boldsymbol{Q}$ (scattering vector) is given by $\boldsymbol{Q} = 4\pi\sin\theta/\lambda$, with $\boldsymbol{Q}$ being the resulting vector between the incoming wave vector $\vec{\boldsymbol{k}}_i$ and the scattered wave vector $\vec{\boldsymbol{k}}_s$, and λ being the neutron wavelength, while θ represents the angle of incident beam. The correlation $d = 2n\pi/Q_n$ is used to calculate the repeat distance (periodicity) d of a lamellar phase from the positions of a series of equidistant peaks Q_n, where n is the diffraction order of the peak.

The commonly applied procedure for the interpretation of neutron diffraction data in order to gain insight into the nano-scaled structure of the model membrane is to calculate the neutron scattering length density (NSLD) profiles $\rho_s(x)$ by a Fourier synthesis of the structure factors F_h according to:

$$\rho_s(x) = a + b\,\frac{2}{d}\sum_{h=1}^{h_{max}} F_h \cos\left(\frac{2\pi h x}{d}\right) \quad (1)$$

In this equation, a and b are unknown coefficients for the relative normalization of $\rho_s(x)$, d is the lamellar periodicity and h the order of diffraction. The absolute value of F_h was calculated by $|F_H| = \sqrt{hI_hA_h}$, where h is the Lorentz correction, A_h is the absorption correction[25] and I_h is the integrated intensity of the h^{th} peak. To calculate $\rho_s(x)$, at least three to four diffraction orders h of one lamellar phase are required. Well-oriented model membranes are essentially needed to record diffraction peaks of higher orders which, however, can be hampered by the poor signal-to-noise (s/n) ratio resulting from the strong background due to the large incoherent scattering cross-section of the large number of hydrogen atoms present in the hydrocarbon chains of SC lipids. Raw data treatment and data reduction to intensity *vs.* 2θ were performed with the *Large Array Manipulation Program* (LAMP, a software package provided by the ILL[26]). Integration of the Bragg peaks, determination of the peak positions and intensities after background subtraction were performed using the software package IGOR Pro 6.1 (WaveMetrics Inc., Portland, OR, USA).

For the Fourier transform, not only the amplitude but also the phase of each F_h is required. With a Gaussian water distribution assumed to feature a maximum at the position $x = d/2$ (near the hydrophilic head group region), the phase of F_h can be determined using the *isomorphous replacement method* described previously.[25,27] Since the lamellar lipid arrangement of the SC model membrane investigated here is supposed to be centrosymmetric, the phase problem simplifies to the possibilities +

or − for the phases of F_h and can be solved by measuring the samples at least at three different D_2O/H_2O ratios. A detailed description of this procedure (so-called contrast variation) and of the neutron diffraction data evaluation can be found elsewhere.[22,25,28]

2.4. ^{2}H NMR experiment

Static ^{2}H NMR spectra were recorded on a Bruker Avance 750 MHz NMR spectrometer (Bruker Biospin GmbH, Rheinstetten, Germany) operating at a resonance frequency of 115.1 MHz for ^{2}H using a single-channel solids probe equipped with a 5 mm solenoid coil. The ^{2}H NMR spectra were accumulated using quadrature phase detection with a phase-cycled quadrupolar echo sequence.[29] The spectral width was set to ±250 kHz. Typical length of a 90° pulse was 3 to 5 μs, and a relaxation delay of 0.8 s or 3 s was applied. The spectra were acquired at temperatures of 32 °C and 80 °C.

The obtained ^{2}H NMR powder spectra of stearic acid (SA-d_{35}) were depaked[30] (using the algorithm of McCabe and Wassall[31]) and the order parameter profiles of the acyl chain were determined from the observed quadrupolar splitting $\Delta\nu_Q(n)$:

$$\Delta\nu_Q(n) = \frac{3}{4}\frac{e^2qQ}{h}S(n) \qquad (2)$$

where e^2qQ/h is the quadrupolar-coupling constant (167 kHz for ^{2}H in a C–^{2}H bond) and $S(n)$ the chain order parameter for the n^{th} carbon position in the chain. Details about the analysis of ^{2}H NMR spectra are found in the literature.[32]

3. Results and discussion

3.1. Neutron diffraction experiments on CER[NP]/cholesterol/stearic acid

Fig. 2 displays the diffraction pattern for the sample CER[NP]/CHOL/SA (55/25/20, m/m) recorded at 100% D_2O contrast and at three different measurement conditions. At 32 °C and 58% RH, obviously two lamellar phases coexist, which are referred to as PI and PII. Five orders of diffraction were detectable for each phase, which differ in their peak shape. The reflections of PI are

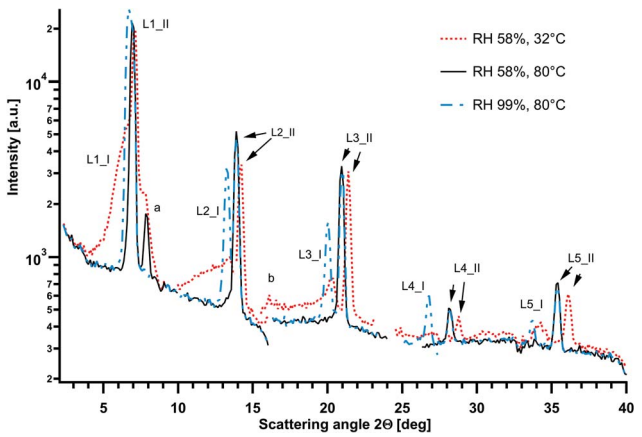

Fig. 2 Neutron diffraction patterns recorded for the ternary sample CER[NP]/CHOL/SA at a D_2O contrast of 100% and different experimental conditions: at 32 °C, 58% RH (red dotted lines), at 80 °C, 58% RH (black solid lines), and 80 °C, 99% RH (blue dash-dotted lines).

smeared-out, broad, and less intense, while the diffraction signals attributed to PII are well defined and sharp. As displayed in Table 1, the lamellar repeat distances d are equal to 39.9 ± 0.3 Å for PI, and 38.2 ± 0.1 Å for PII, respectively. Peaks located at $2\theta = 7.8°$ and 16° are attributed to segregated crystalline CHOL, whose occurrence was already described before and is known to not affect the lamellar order of the model membranes.[20,33,34] From these first findings, we conclude a certain fraction of SC lipids to be sequestered into the additionally occurring lamellar phase PII. However, at 80 °C and 58% RH, only the peaks attributed to PII are detectable, while PI disappears (see Fig. 2). Simultaneously, PII *increases* its d-spacing by 0.7 Å to 38.9 Å (Table 1), recognizable by a shift of the diffraction signals towards lower 2θ values. Phase-separated CHOL is still detectable. When the relative humidity is subsequently raised to 99% while the temperature is kept at 80 °C, two coexisting phases are formed again. The reappearing phase is clearly pronounced and exhibits sharp diffraction signals of high intensity up to the 5th order. However, the lamellar repeat distance is increased by 1.2 Å when compared to the phase PI at lower temperature. Phase-separated CHOL is no longer observed, indicating an improved miscibility of this rigid molecule with the other SC lipids at high temperature and high humidity. This can be explained with the increased area per SC lipid molecule due to enhanced head group hydration at higher humidity, which allows for improved CHOL incorporation into the SC lipid lamellae. Under all experimental conditions studied, the lamellar phase PII did neither disappear, nor show any clear response to D_2O contrast variation, *i.e.* the diffraction intensity was not dependent on the D_2O/H_2O ratio (diffraction patterns not shown). In contrast, PI was found to exhibit the expected response to D_2O contrast variation. Two conclusions can be drawn from these experimental findings: first, the SC lipids arranged in PII presumably are virtually shielded from any interactions with the water vapour, which prevents appreciable interlamellar hydration. This does not apply for the SC lipids assembled in PI. Consequently, the lipid arrangement must differ in both phases. Second, temperature-dependent reorganization of the lipid lamellae takes place. One phase, PI, is no longer detectable at 80 °C, while PII persists, but slightly increases its repeat distance. The latter is an atypical behaviour. Usually, the lamellar spacing of phospholipid bilayers *decreases* at high temperature due to an increased number of *gauche* defects, increased chain fluidity and consequently stronger interdigitation.[35,36] Such an expected behaviour with decreased bilayer repeat distance at higher temperature was also observed before for SC model membranes based on the more polar CER[AP].[37]

Table 1 Lamellar d-spacings of the ternary model membrane composed of CER[NP], CHOL and SA (mass ratio 55/25/20) calculated from the neutron diffraction data. Measurements were carried out at 32 °C or 80 °C, and at RH 58% or 99%. The values for d given in Å are averaged over three D_2O concentrations (n.d.: not detectable)

	58% RH		99% RH	
Temperature	PI	PII	PI	PII
32 °C	40.0 ± 0.1	38.2 ± 0.1	39.9 ± 0.3	38.2 ± 0.1
80 °C	n.d.	38.9 ± 0.1	41.1 ± 0.2	38.9 ± 0.1

Since PII did not display considerable contrast variation and the F_h amplitudes do not display changes beyond statistical uncertainty at increasing D_2O concentrations (see Table 2), we cannot determine the F_h signs for PII reliably. However, since there is at least a tendency we assume the signs for the diffraction orders 1–5 as − + − + −. The $\rho_s(x)$ received from Fourier synthesis are shown in Fig. 3. In general, a typical bilayer arrangement can be deduced from the calculated profiles. Both, PI and PII exhibit two maxima at the outer edges of the $\rho_s(x)$, which indicate the presence of molecular groups with a positive neutron scattering length, *i.e.* the head groups of SA and CER [NP]. In the central bilayer region at $x = 0$ Å, both profiles exhibit minima, indicating a high density of atoms with negative neutron scattering length (*i.e.* the methylene groups and terminal methyl groups of the lipid alkyl chains). The shape of the membrane profile with the maxima located at $x_{PH} = d/2$ suggests a very small intermembrane space with a thin water layer present as reported previously.[18] The latter preferentially applies for PI, whose head group region features maxima with different intensities at the three D_2O contrasts studied (Fig. 3A). In contrast, the insensitivity of the head group region of PII to D_2O contrast variation becomes apparent in the stable maxima of the $\rho_s(x)$, suggesting the absence of exchanged deuterium in that region, and consequently the absence of interlamellar water (Fig. 3B). To further underline this finding, we calculated the water distribution $\rho_w(x)$ across the lamellar unit cell according to ref. 18 for both PI and PII using eqn (3):

$$\rho_w(x) = \rho_{50\%D_2O} - \rho_{8\%D_2O} \quad (3)$$

The $\rho_w(x)$ presented in Fig. 3C prove that there is practically no water present in the interlamellar space of PII. Accordingly, the observed increase of d for PII at 80 °C does not result from swelling. In contrast, the two maxima in $\rho_w(x)$ of PI reveal the presence of a certain amount of free water in the head group region exchanged by D_2O. These findings underline the completely different hydration characteristics of PI and PII. However, it remains unclear from the present data whether a considerable interlamellar hydration of PII is possible after a longer equilibration time, *e.g.* several days.

Taking into account former reports in the literature, it is most likely that PII is constituted by crystalline phase-separated CER [NP]. Raudenkolb *et al.* investigated pure CER[NP] in water by X-ray diffraction and reported almost identical lamellar spacings and temperature-dependent changes,[13] as we observed for PII. Although several studies proved that ternary systems of CER[NP], CHOL and free fatty acid are well miscible,[15,38] we assume that PII is exclusively formed by segregated ceramide. However, the incorporation of a certain amount of CHOL into the lamellar phase PII cannot be ruled out from the experimental diffraction data. In order to definitely elucidate this, the application of specifically deuterated SC lipids might be helpful. As shown previously,[23,39,40] selective deuterium labelling allows for the direct localization of the deuterated compounds inside the model bilayers. The coexisting phase PI at 32 °C could either be phase-separated fatty acid,[41] or is made up of SA besides the other membrane components. In the first case, the observed formation of a one-phase system at 80 °C and 58% RH would originate from fluidization of the SA-rich phase and subsequent melting (melting point of SA: about 68 °C[38]). In the latter case, an improved miscibility of the SC lipids at increased temperature could account for the formation of one single phase at 80 °C and 58% RH.

In the remaining lamellar arrangement of PII, the rigid and lipophilic CER[NP] forms the stabilizing bilayer backbone. Former reports regarding the water impermeability of films composed of CER[NP],[16] and the inaccessibility of the head group region for deuterium exchange[14] may confirm the assumption of pure CER[NP] constituting PII, and corroborate our experimental finding of lacking contrast variation in that phase. A possible explanation is provided by the results of Dahlen and Pascher[42] who stated a V-shaped CER conformation for *N*-tetracosanoyl-phytosphingosine with the alkyl chains of asymmetric length pointing in opposite directions and the hydrophilic head group being located in the apex of the angle of 101°. Such a structural conception based on CER[NP] outstretching its two alkyl chains in opposite directions is likewise possible for PII of the ternary model membrane studied here and would explain the lacking contrast variation, with the small ceramide head group shielded from hydration by the outstretched alkyl chains and by the inter- and intramolecular network of hydrogen bonds described for phytosphingosine-type CERs.[43,44] The lacking response of PII to D_2O contrast variation has not been reported before for the CER[AP]-based,[41] or other CER-based SC lipid model membranes. We therefore conclude that the respective CER species present in the model system influences the lamellar structure and the SC lipid arrangement to a high extent. In addition, the V-shaped CER conformation could also account for the slightly larger d-spacing of PII at 80 °C by expansion of the chain angle.[13]

Due to the low affinity of CER[NP] based model membranes to water, it seems likely that the more humid vapour of 99% RH

Table 2 The amplitudes of the structure factors F_h calculated for PII of the multilamellar sample containing CER[NP], CHOL and SA (mass ratio 55/25/20) at 32 °C and 58% RH

	8% D_2O		50% D_2O		100% D_2O	
Diffraction order	Structure factor	Error	Structure factor	Error	Structure factor	Error
L1	74.16	0.35	73.36	0.23	71.60	0.12
L2	44.83	0.73	45.80	0.55	44.10	0.46
L3	50.82	0.92	50.79	0.89	49.74	0.28
L4	17.50	1.13	17.93	1.03	16.45	0.62
L5	24.91	1.14	24.42	0.95	24.66	0.82

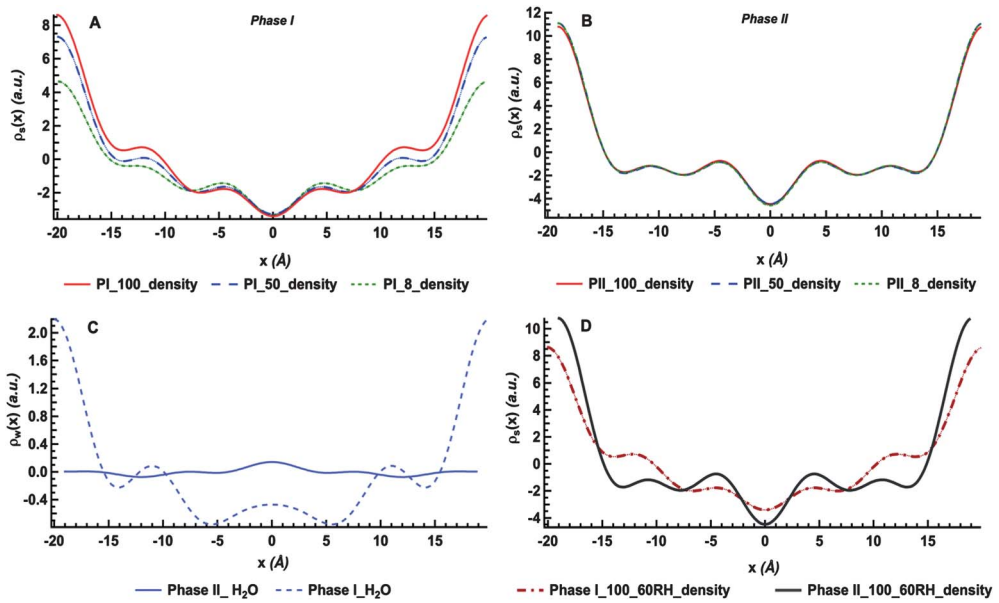

Fig. 3 The calculated NSLD profiles for PI (A) and PII (B) at 32 °C, 58% RH, and 100% (red solid line), 50% (blue dashed line), 8% (green dotted line) D_2O. Note the varying amplitude of the two maxima located at the outer edges in the case of PI (A), which is not observed for PII (B). (C) Water density distribution profile across the membrane for PI (blue dashed line) and PII (blue solid line). (D) Parallel presentation of NSLD profiles for PI (red dash-dotted line) and PII (black solid line) after F_h normalization to 1. Experimental conditions are equivalent (100% D_2O, 32 °C, 58% RH).

induces a distinct hydration pressure to the SC lipids assembled in PII. This would provide a possible explanation for the observed reversible segregation of PI at 80 °C and 99% RH. While presumably a large fraction of CER[NP] remains as PII being still inaccessible for hydration, at least a part of the ceramide and the other model membrane components with a higher affinity to hydration, particularly the fatty acid, presumably form the re-appearing lamellar phase PI at 80 °C and 99% RH. Fig. 4 displays a sketch of the assumed SC lipid assembly of PI and PII at 80 °C and RH 99%. The well-defined diffraction peaks and the state of high lamellar order of PI despite the high temperature suggest that a certain amount of CER[NP] is incorporated into this phase besides CHOL and SA. The repeat distance is increased by about 1 Å in comparison to PI at 32 °C, and D_2O contrast variation results in increasing structure factor amplitudes. This finding indicates that the interlamellar space is hydrated to a certain extent in this phase. In order to allow for such a hydration, the ceramide molecules need to exhibit a less densely packed assembly in comparison to PII. This could be possible due to a significantly weakened hydrogen bond network of the ceramide head group at higher temperature. At this point, it is not clear whether a chain flip resulting in a hair-pin conformation of the ceramide molecules being reported before for the related phytosphingosine-based CER[AP] under excess water[17,18] is likewise possible for CER[NP]. However, at 80 °C and excess hydration, significant changes in the lateral packing behaviour of the CER[NP] were reported previously with reorganization from orthorhombic to hexagonal chain packing. It was concluded that changes in the hydrogen bond network account for these changes.[16] These findings may explain the re-occurrence of a stable and well-ordered lamellar phase at high temperature and high humidity, as reported in the present work.

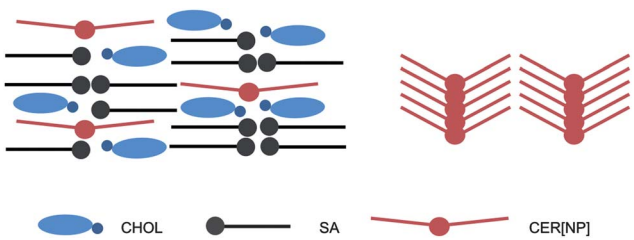

Fig. 4 Sketch of the assumed lamellar lipid assembly present in the phase-separated domains of PI and PII in the ternary SC lipid model membrane containing CER[NP], CHOL and SA at 80 °C and 99% RH. While PII is constituted by crystalline CER[NP] showing a V-shaped conformation, PI is formed by CER[NP], SA and CHOL.

To summarize, we observed a stable and dense bilayer assembly with surprising characteristics upon hydration and heating which suggest a V-shaped CER conformation, and co-existence of two lamellar phases. The distinct properties of CER [NP] probably account for the poorly hydrated but highly ordered bilayer organization present in the investigated SC lipid model membrane. From these findings, we conclude a protruding influence of the phytosphingosine-type ceramides for the proper formation of a stable SC bilayer structure.

3.2. ^{2}H NMR spectroscopy on CER[NP]/cholesterol/stearic acid and CER[AP]/cholesterol/stearic acid

The morphology of the bilayer structure in the presence of CER [NP] was further corroborated by ^{2}H NMR spectroscopy on either perdeuterated SA-d_{35} or partially deuterated cholesterol-d_7 in the ternary mixtures. Typical ^{2}H NMR spectra are shown in Fig. 5. In the CER[NP] containing mixture, the ^{2}H NMR

spectrum of stearic acid shows the typical superposition of Pake doublets indicative of a lamellar and fluid phase state at 80 °C (A) and mainly 32 °C (B). However, at a temperature of 32 °C some molecules in the CER[NP] mixture are in the ordered phase as indicated from a broad plateau underneath the spectrum with a width of approximately ±65 kHz. The ^{2}H NMR spectrum of cholesterol-d_7 (C) is dominated by a narrow quadrupolar splitting from the two methyl groups at C26 and C27 and a larger splitting coming from the deuteron attached to C25.

In the CER[AP] containing mixture, the ^{2}H NMR spectrum of stearic acid at 32 °C (E) represents the superposition of a highly ordered phase with part of the molecules in a more fluid state, however, not comparable to a true liquid-crystalline phase state as shown at 80 °C (D). As again can be seen from a broad plateau underneath the spectrum some molecules are in an ordered phase in the CER[AP] mixture even at the high temperature. The ^{2}H NMR spectrum of cholesterol-d_7 is again very similar to that in the ternary mixture with CER[NP].

The ^{2}H NMR spectra do not show any indications that either SA or cholesterol would be present in more than just one phase. If either of the molecules was contained in both the PI and the PII phases, we would have detected two sets of quadrupolar splittings for each deuteron, which was clearly not the case but has been described in the literature.[45–47] This supports the model that attributes stearic acid and cholesterol to one of the lamellar phases, PI, with no exchange between the two phases (see Fig. 4). While the cholesterol spectra are identical in both mixtures, the ones attributed to the stearic acid vary more significantly between the two systems. Presumably, the structural assembly of the fatty acid is affected to a higher extent by the respective CER species, than the cholesterol. While CER[NP] appears to prefer a fluid phase state, the CER[AP] stabilizes a more rigid gel-like state. This reflects the structural differences of the two molecules.

More structural insights into the PI phase can be obtained from the analysis of the order parameter profiles derived from the ^{2}H NMR spectra of SA-d_{35}, which are shown in Fig. 6. All order parameters are relatively high and thus indicative of a tightly packed lamellar structural arrangement. This supports the results received from the neutron diffraction experiments and underlines the high state of lamellar order, which is based on the presence of the CER species. Although the mixture containing CER[AP] appears to stabilize the gel state, at 80 °C it shows lower order parameters than the mixture containing CER[NP]. Highest order parameters are shown for the CER[NP] containing mixture at 32 °C, while the corresponding spectrum of the CER [AP] containing mixture could not be analysed due to the high proportion of a gel state.

Significantly increased order parameters were measured for SA-d_{35} in the mixture containing CER[NP] compared to CER [AP]. The reason for the higher state of order in the presence of CER[NP] compared to the ternary system composed of CER [AP] could be the α-hydroxyl group present in the amide bound stearic acid of CER[AP]. Although phytosphingosine-based ceramides are known to form a strong inter- and intra-molecular hydrogen bond network, also the localization of the hydroxyl groups involved in this network plays a crucial role: while the vicinal hydroxyl groups of CER[NP] and CER[AP] are important for the formation of intermolecular interactions, the α-hydroxy group only present in CER[AP] was found to somehow weaken the head group interaction between the SC lipids.[48] This influence was corroborated by the ^{2}H NMR results since the order parameter profiles show higher order parameters for the CER[NP] based model system (Fig. 6).

The NMR order parameters further allow the calculation of geometric parameters for the molecular packing in phase PI (see Table 3).[49] The stearic acid chains are very much elongated requiring a minimal cross-sectional area in the mixture with CER [NP]. In the mixture with CER[AP], the stearic acid chains are more disordered, however, they still represent a rigid extended conformation. From these geometrical parameters, the fraction of *gauche* conformers in each chain can be calculated[50] and is also given in Table 3. In the most rigid conformation, stearic acid on average only features ~2.2 *gauche* defects, which agrees with a very well ordered free fatty acid. This all confirms the model, according to which the stearic acid is forced into a more rigid and ordered structure when CER[NP] is present: the longer alkyl

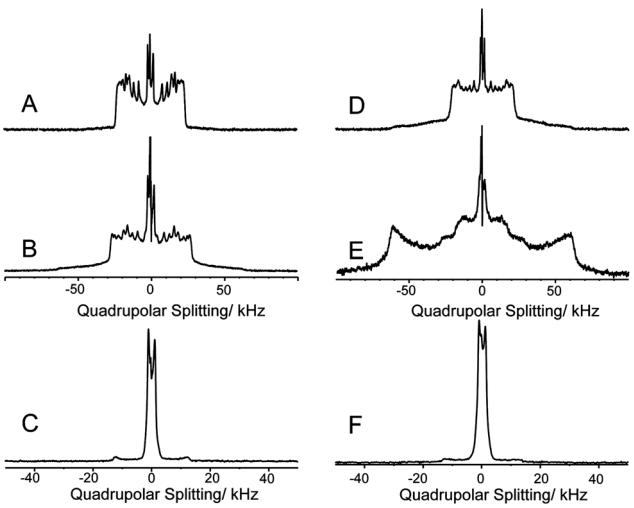

Fig. 5 ^{2}H NMR spectra of CER[NP]/CHOL/SA-d_{35} at 80 °C (A) and 32 °C (B), CER[NP]/CHOL-d_7/SA at 80 °C (C), CER[AP]/CHOL/SA-d_{35} at 80 °C (D) and 32 °C (E), CER[AP]/CHOL-d_7/SA at 80 °C (F).

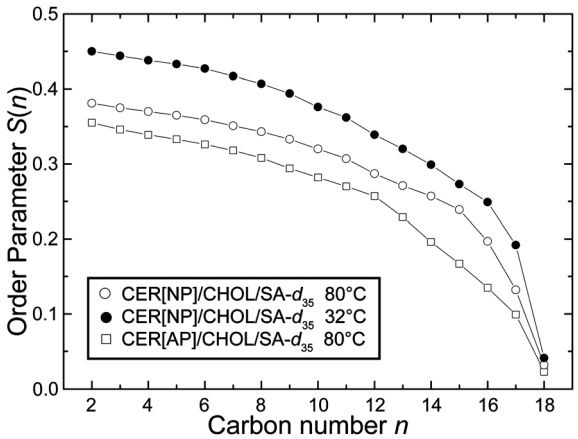

Fig. 6 Order parameter profiles obtained from the ^{2}H NMR spectra for the stearic acid in CER[NP]/CHOL/SA-d_{35} and in CER[AP]/CHOL/SA-d_{35} at a temperature of 32 °C and 80 °C.

Table 3 Calculated geometric parameters: mean interfacial area of one chain (A) and the chain extent (L_c[a]) for the deuterated hydrocarbon chain of SA in the investigated samples

	T/°C	A/Å^2	L_c[a]/Å	*Gauche* conformers per chain
NP/CHOL/SA-d_{35}	80	25.2	16.8	3.2
	32	22.5	17.9	2.2
AP/CHOL/SA-d_{35}	80	25.9	15.9	4.0
	32	—[a]	—[a]	—[a]

[a] Parameters could not be calculated due to the presence of the gel phase state.

chain extent indicates the prevalence of *trans* conformers, and the smaller area per molecule likewise suggests a more dense packing in comparison with the CER[AP] based system.

In conclusion, SA-d_{35} experiences a distinct influence from the respective CER species present in the mixture. This furthermore supports our assumption considering the molecular arrangement of the SC lipids in this model system based on a V-shaped conformation of CER[NP].

4. Conclusions

The present study investigated ternary SC lipid models containing the phytosphingosine-based CER[NP], CHOL and the fatty acid SA. We explored the influence of this sphingolipid species on the lamellar lipid assembly and investigated the samples by means of neutron diffraction and ^{2}H NMR spectroscopy. Our results indicate that in the presence of CER[NP], phase separation occurs, and a highly ordered lamellar SC model system is formed. Even at high temperature, the system exhibits bilayers with a densely packed and stable lamellar backbone. From the present data, we conclude that the phytosphingosine-type CER[NP] exerts a dominating influence on the structure of the ternary SC model: it prevents the model membrane from significant hydration and swelling, probably due to intense intra- and intermolecular head group interactions. Furthermore, it appears that model membranes based on CER[NP] exhibit a completely different temperature-dependent behaviour and different hydration characteristics, when compared to the closely related CER[AP] described in preceding studies.[37,41] Thus, the CER head group apparently has a significant influence on the arrangement of the membrane lipids. The absence of only one OH group in the CER molecule leads to drastic structural changes as reported here. The interdisciplinary approach of our present study highlights the importance of applying combined techniques in order to elucidate the influence of particular CER species on the structural arrangement of simplistic SC lipid model membranes.

Abbreviations

SC	Stratum corneum
CER	Ceramide
CER[NP]	*N*-(Nonhydroxyoctadecanoyl)-phytosphingosine
CER[AP]	*N*-(α-Hydroxyoctadecanoyl)-phytosphingosine
CER[EOS]	30-Linoyloxy-triacontanoic acid-[(2*S*,3*R*)-1,3-dihydroxyocta-dec-4-enyl]-amide
FFA	Free fatty acid
SA	Stearic acid
CHOL	Cholesterol
NSLD	Neutron scattering length density
RH	Relative humidity

Acknowledgements

The authors would like to express their gratitude to Evonik Goldschmidt GmbH (Essen, Germany) for the donation of CER [NP] and CER[AP]. T. Engelbrecht would like to thank the Graduiertenförderung des Landes Sachsen-Anhalt as well as Evonik Goldschmidt for funding. We gratefully acknowledge granting of beam-time and financial assistance by Institute Laue-Langevin (ILL, Grenoble, France). We thank the DFG (German Research Foundation) and the Experimental Physics Institutes of the University of Leipzig for providing measuring time on the Avance 750 MHz NMR spectrometer.

References

1 P. M. Elias, *J. Invest. Dermatol.*, 1983, **80**(suppl), 44s–49s.
2 P. M. Elias, J. Goerke and D. S. Friend, *J. Invest. Dermatol.*, 1977, **69**, 535–546.
3 P. W. Wertz and B. van den Bergh, *Chem. Phys. Lipids*, 1998, **91**, 85–96.
4 G. M. Gray and H. J. Yardley, *J. Lipid Res.*, 1975, **16**, 434–440.
5 G. Brooks and B. Idson, *Int. J. Cosmet. Sci.*, 1991, **13**, 103–113.
6 S. E. Friberg, I. Kayali, W. Beckerman, L. D. Rhein and A. Simion, *J. Invest. Dermatol.*, 1990, **94**, 377–380.
7 P. W. Wertz, *Exog. Dermatol.*, 2004, **3**, 53–56.
8 L. Coderch, O. Lopez, A. de la Maza and J. L. Parra, *Am. J. Clin. Dermatol.*, 2003, **4**, 107–129.
9 G. Imokawa, A. Abe, K. Jin, Y. Higaki, M. Kawashima and A. Hidano, *J. Invest. Dermatol.*, 1991, **96**, 523–526.
10 A. Di Nardo, P. Wertz, A. Giannetti and S. Seidenari, *Acta Derm.-Venereol.*, 1998, **78**, 27–30.
11 S. Motta, M. Monti, S. Sesana, R. Caputo, S. Carelli and R. Ghidoni, *Biochim. Biophys. Acta*, 1993, **1182**, 147–151.
12 S. Raudenkolb, W. Hubner, W. Rettig, S. Wartewig and R. H. H. Neubert, *Chem. Phys. Lipids*, 2003, **123**, 9–17.
13 S. Raudenkolb, S. Wartewig and R. H. H. Neubert, *Chem. Phys. Lipids*, 2003, **124**, 89–101.
14 M. E. Rerek, H. C. Chen, B. Markovic, D. Van Wyck, P. Garidel, R. Mendelsohn and D. J. Moore, *J. Phys. Chem. B*, 2001, **105**, 9355–9362.
15 M. E. Rerek, D. van Wyck, R. Mendelsohn and D. J. Moore, *Chem. Phys. Lipids*, 2005, **134**, 51–58.
16 P. Garidel, *Phys. Chem. Chem. Phys.*, 2002, **4**, 1934–1942.
17 M. A. Kiselev, *Crystallogr. Rep.*, 2007, **52**, 525–528.
18 M. A. Kiselev, N. Y. Ryabova, A. M. Balagurov, S. Dante, T. Hauss, J. Zbytovská, S. Wartewig and R. H. H. Neubert, *Eur. Biophys. J.*, 2005, **34**, 1030–1040.
19 D. Kessner, M. Kiselev, S. Dante, T. Hauss, P. Lersch, S. Wartewig and R. H. Neubert, *Eur. Biophys. J.*, 2008, **37**, 989–999.
20 A. Schröter, D. Kessner, M. A. Kiselev, T. Hauss, S. Dante and R. H. H. Neubert, *Biophys. J.*, 2009, **97**, 1104–1114.
21 M. Seul and M. J. Sammon, *Thin Solid Films*, 1990, **185**, 287–305.
22 D. L. Worcester and N. P. Franks, *J. Mol. Biol.*, 1976, **100**, 359–378.
23 A. Schroeter, M. A. Kiselev, T. Hauss, S. Dante and R. H. H. Neubert, *Biochim. Biophys. Acta, Biomembr.*, 2009, **1788**, 2194–2203.

24 A. Carruthers and D. L. Melchior, *Biochemistry*, 1983, **22**, 5797–5807.
25 N. P. Franks and W. R. Lieb, *J. Mol. Biol.*, 1979, **133**, 469–500.
26 D. Richard, M. Ferrand and G. J. Kearley, *J. Neutron Res.*, 1996, **4**, 33–39.
27 S. Dante, T. Hauss and N. A. Dencher, *Biochemistry*, 2003, **42**, 13667–13672.
28 J. F. Nagle and S. Tristram-Nagle, *Biochim. Biophys. Acta*, 2000, **1469**, 159–195.
29 J. H. Davis, K. R. Jeffrey, M. Bloom, M. I. Valic and T. P. Higgs, *Chem. Phys. Lett.*, 1976, **42**, 390–394.
30 E. Sternin, M. Bloom and A. L. Mackay, *J. Magn. Reson.*, 1983, **55**, 274–282.
31 M. A. McCabe and S. R. Wassall, *J. Magn. Reson., Ser. B*, 1995, **106**, 80–82.
32 D. Huster, K. Arnold and K. Gawrisch, *Biochemistry*, 1998, **37**, 17299–17308.
33 M. R. Ali, K. H. Cheng and J. Huang, *Biochemistry*, 2006, **45**, 12629–12638.
34 V. Pata and N. Dan, *Biophys. J.*, 2005, **88**, 916–924.
35 R. T. Zhang, W. J. Sun, S. Tristram-Nagle, R. L. Headrick, R. M. Suter and J. F. Nagle, *Phys. Rev. Lett.*, 1995, **74**, 2832–2835.
36 F. Y. Chen, W. C. Hung and H. W. Huang, *Phys. Rev. Lett.*, 1997, **79**, 4026–4029.
37 A. Schroeter, *The role of ceramide [AP] for the structural assembly of stratum corneum lipid model membranes*, Ph.D. thesis, Martin Luther University Halle-Wittenberg, 2010.
38 N. Ohta and I. Hatta, *Chem. Phys. Lipids*, 2002, **115**, 93–105.
39 T. N. Engelbrecht, A. Schroeter, T. Hauss and R. H. Neubert, *Biochim. Biophys. Acta, Biomembr.*, 2011, **1808**, 2798–2806.
40 D. Kessner, M. A. Kiselev, T. Hauss, S. Dante, S. Wartewig and R. H. Neubert, *Eur. Biophys. J.*, 2008, **37**, 1051–1057.
41 A. Ruettinger, M. A. Kiselev, T. Hauss, S. Dante, A. M. Balagurov and R. H. Neubert, *Eur. Biophys. J.*, 2008, **37**, 759–771.
42 B. Dahlen and I. Pascher, *Acta Crystallogr., Sect. B: Struct. Crystallogr. Cryst. Chem.*, 1972, **28**, 2396–2404.
43 P. Garidel, B. Folting, I. Schaller and A. Kerth, *Biophys. Chem.*, 2010, **150**, 144–156.
44 I. Pascher, *Biochim. Biophys. Acta*, 1976, **455**, 433–451.
45 A. Bunge, P. Müller, M. Stöckl, A. Herrmann and D. Huster, *Biophys. J.*, 2008, **94**, 2680–2690.
46 T. Bartels, R. S. Lankalapalli, R. Bittman, K. Beyer and M. F. Brown, *J. Am. Chem. Soc.*, 2008, **130**, 14521–14532.
47 S. L. Veatch, O. Soubias, S. L. Keller and K. Gawrisch, *Proc. Natl. Acad. Sci. U. S. A.*, 2007, **104**, 17650–17655.
48 E. Corbe, C. Laugel, N. Yagoubi and A. Baillet, *Chem. Phys. Lipids*, 2007, **146**, 67–75.
49 A. Vogel, C. P. Katzka, H. Waldmann, K. Arnold, M. F. Brown and D. Huster, *J. Am. Chem. Soc.*, 2005, **127**, 12263–12272.
50 A. Vogel, G. Reuther, K. Weise, G. Triola, J. Nikolaus, K. T. Tan, C. Nowak, A. Herrmann, H. Waldmann, R. Winter and D. Huster, *Angew. Chem., Int. Ed.*, 2009, **48**, 8784–8787.